**Atmospheric
Measurement
Techniques
Discussions**

Retrieval of MetOp-A/IASI CO profiles and validation with MOZAIC data

E. De Wachter[1], B. Barret[1], E. Le Flochmoën[1], E. Pavelin[2], M. Matricardi[3], C. Clerbaux[4,5], J. Hadji-Lazaro[4], M. George[4], D. Hurtmans[5], P.-F. Coheur[5], P. Nedelec[1], and J. P. Cammas[1]

[1]Laboratoire d'Aérologie-OMP, UMR5560, CNRS-Université de Toulouse, Toulouse, France
[2]Met Office, Exeter, UK
[3]ECMWF, Reading, UK
[4]UPMC Univ. Paris 06; Université Versailles St-Quentin; CNRS/INSU – UMR8190, LATMOS-IPSL, Paris, France
[5]Spectroscopie de l'Atmosphère, Chimie Quantique et Photophysique, Université Libre de Bruxelles, Bruxelles, Belgium

Correspondence to: E. De Wachter (wace@aero.obs-mip.fr)

Discussion Paper | **Discussion Paper** | **Discussion Paper** | **Discussion Paper**

Abstract

The IASI nadir looking thermal infrared sounder onboard MetOp-A enables the monitoring of atmospheric constituents on a global scale. This paper presents a quality assessment of IASI CO profiles retrieved by the two different retrieval algorithms SOFRID and FORLI, by an intercomparison with airborne in-situ CO profiles from the MOZAIC program. A statistical analysis shows a very good agreement between the two retrieval algorithms and smoothed MOZAIC data for the lower troposphere (surface-480 hPa) with correlation coefficients $r \sim 0.8$, and a good agreement in the upper troposphere (480–225 hPa) with $r \sim 0.7$. Closer investigation of the temporal variation of the CO profiles at the airports of Frankfurt and Windhoek demonstrates that on the overall a very good agreement is found between the IASI products and smoothed MOZAIC data in terms of seasonal variability. At Frankfurt SOFRID (resp. FORLI) is positively biased by 10.5 % (resp. 13.0 %) compared to smoothed MOZAIC in the upper (resp. lower) troposphere, and the limited sensitivity of the IASI instrument to the boundary layer when thermal contrast is low is identified. At Windhoek, we find a good reproduction of the impact of the vegetation fires in Southern Africa from July to November by both SOFRID and FORLI, with an overestimation of the CO background values (resp. fire maxima) by SOFRID (resp. FORLI) by 12.8 % (resp. ~10 %). Profile comparisons at Frankfurt and Windhoek identify a reduced performance of the nighttime retrievals of both products compared to daytime retrievals.

1 Introduction

Carbon monoxide (CO) is primarily produced at the surface by biomass burning and fossil fuel combustion. In the atmosphere, oxidation of methane (CH_4) and non-methane hydrocarbons (NMHC), like isoprene, account for nearly half of the global CO production (Brenninkmeijer and Novelli, 2003). Sources of secondary importance include emission by vegetation and oceans. The removal of CO is largely (for as much

as 90 %) determined by the reaction with the hydroxyl (OH) radical. The remaining 10 % is removed by soils (Brenninkmeijer and Novelli, 2003).

Although not considered as a greenhouse gas, CO has a strong indirect effect on the radiation balance of the atmosphere. Through its reaction with OH, CO largely determines the oxidizing capacity of the atmosphere, thereby having a strong impact on the lifetimes of long-lived trace gases (Bergamaschi et al., 2000). Furthermore, being involved in the production and destruction of ozone (O_3), O_3-CO correlation studies can provide important insight into the photochemical origin of air masses (Parrish et al., 1993; Chin et al., 1994; Voulgarakis et al., 2011). In addition, having a lifetime in the troposphere of 1–2 months, CO is an excellent tracer to study the long-range transport of pollution (Logan et al., 1981; Forster et al., 2001).

Thermal infrared (TIR) nadir sounders are particularly suited for vertical profiling of atmospheric trace gases with a high spatial resolution. IASI, the Infrared Atmospheric Sounding Interferometer, onboard MetOp-A, is dedicated to long-term global scale monitoring of a series of key atmospheric species, with unprecedented spatial sampling and coverage (Clerbaux et al., 2009). Laboratoire d'Aérologie (LA) and LATMOS/Université Libre de Bruxelles (ULB) deliver profiles of atmospheric CO based on two different retrieval algorithms: the SOftware for a Fast Retrieval of IASI Data (SOFRID), and the Fast Optimal Retrievals on Layers for IASI (FORLI). This paper provides a comparison of the CO products obtained by the two algorithms with high precision airborne in-situ CO observations from the Measurements of OZone, water vapour, carbon monoxide and nitrogen oxides by Airbus In-service airCraft (MOZAIC) program (Marenco et al., 1998).

The SOFRID algorithm was developed at LA for the fast retrieval of O_3 and CO profiles on a global scale from IASI spectra. Barret et al. (2011) showed that tropospheric SOFRID O_3 profiles can be retrieved with almost 2 independent pieces of information, the tropospheric ozone column (surface-225 hPa) and the upper tropospheric-lower stratospheric (UTLS) column (225–70 hPa), with errors smaller than 20 %. Given the great value of coexistent observations of O_3 and CO on a global scale, SOFRID has

been expanded to allow the retrieval of CO profiles. Our goal is to describe the SOFRID CO retrieval in detail and assess the quality of the retrieved profiles through a comparison with MOZAIC aircraft data.

The FORLI algorithm (Hurtmans et al., 2012) provides daily retrievals of CO, O_3 and
5   HNO_3. The FORLI CO product comprises CO total columns, partial columns, profiles, quality flags and the corresponding averaging kernel vector or matrix. It has undergone a series of quality assessments. George et al. (2009) evaluated global distributions of FORLI CO total columns with the nadir-looking TIR instruments MOPITT, AIRS and TES. A qualitative analysis of the FORLI retrieved CO profiles was made by Turquety
10 et al. (2009) by analysing the performance of the CO retrievals during extreme fire events. Pommier et al. (2010) compared total columns, 0–5 km partial columns and profiles with collocated aircraft observations in the Arctic during the spring and summer 2008 POLARCAT campaigns. This study complements the previous works by validation of FORLI CO profiles against the MOZAIC 2008–2009 dataset. As the FORLI
15 CO products will be operationally distributed in 2013 through the EUMETCast system (under the O3MSAF umbrella) this paper is an important step to evaluate the quality of the CO profile data before widespread distribution.

The paper is structured as follows: In the following section we introduce the two algorithms developed to retrieve CO profiles from IASI radiances. Section 3 presents
20 the MOZAIC reference data set used in the validation study and in Sect. 4 the validation methodology and results are discussed. The conclusion is given in Sect. 5.

2   Retrieval from MetOp-A/IASI radiances

2.1   IASI

IASI is one of the 12 instruments onboard MetOp-A, the first of a series of successive
25 polar-orbiting satellites. Launched in October 2006, IASI is a Fourier Transform Spectrometer (FTS), designed to measure the infrared (IR) spectrum emitted by the Earth

and the atmosphere, from 645 to 2760 cm^{-1}, with a spectral resolution of 0.5 cm^{-1} after apodisation. As compared to other TIR sounders in orbit, IASI offers a large and continuous spectral coverage of the IR region at a medium spectral resolution (Clerbaux et al., 2009). It provides global Earth coverage twice a day, with an overpass time at ~09:30 and ~21:30 LT (local time), and a relatively small pixel size on the ground (12 km at nadir).

IASI's objectives are the delivery of highly accurate meteorological products to help improve operational weather predictions, as well as the monitoring of reactive gases on a global scale.

2.2 SOFRID

The SOFRID algorithm aims at a fast retrieval of global O$_3$ and CO from MetOp/IASI radiances. It is based on the RTTOV fast radiative transfer model coupled to a 1D-Var retrieval scheme. The retrieval of SOFRID O$_3$ profiles is described in detail in Barret et al. (2011) and a validation study with ozonesondes is given by Dufour et al. (2012). For this validation study SOFRID v2.0 was used.

The UKMO 1D-Var algorithm (Pavelin et al., 2008) is a retrieval code for nadir-viewing passive sounding satellites, developed at UK Met Office within the context of the EUMETSAT Satellite Application Facility for Numerical Weather Prediction (NWP SAF). It is based on the optimal estimation method (OEM) described by Rodgers (2000). In the OEM an optimal solution is found given the measurement, a simulation of the observed radiance, the a priori information and associated errors. Hence, an accurate radiative transfer model and a representative set of a priori assumptions and their uncertainties need to be provided.

The radiative transfer calculations are performed with the RTTOV-9.3 model (Saunders et al., 1999; Matricardi et al., 2004; Matricardi, 2009). RTTOV is a regression model where optical depths are parameterised by a set of predefined profile dependent-predictors, which are functions of temperature, pressure, absorber amount

and viewing angle (Matricardi et al., 2004). The RTTOV regression coefficients are derived from accurate line-by-line calculations performed with the line-by-line radiative transfer model (Clough et al., 2005) using molecular data from the HITRAN 2004 spectroscopic database (Rothman et al., 2005). The land emissivity is calculated with

5   the RTTOV UWiremis IR land surface emissivity module (Borbas and Ruston, 2010). Surface pressure, temperature and humidity profiles for the radiative calculations are taken from the operational MetOp-A Level 2 (L2) IASI product (Schlüssel et al., 2005). Surface temperature, skin temperature and wind speed are provided by the European Centre for Medium-range Weather Forecasts (ECMWF).

10   SOFRID CO retrievals are calculated from radiances in the 2143–2181 cm^{-1} spectral window and are retrieved on 43 fixed pressure levels from the surface up to 0.1 hPa. The covariance of the measurement error is characterized by a 5-band matrix (i.e. a pentadiagonal matrix, which is representative for apodised observations) with a radiometric noise set to 1.41×10^{-8} W$(\text{cm}^2\,\text{sr}\,\text{cm}^{-1})^{-1}$. This value is the so-called obser-

15   vational error, including not only the measurement error, but also the uncertainties in the temperature and water vapor profile, the spectroscopic parameters and surface emissivity.

The a priori information was build from a 2 yr dataset of MOZAIC aircraft CO profiles, complemented by Aura/MLS profiles at altitudes higher than the aircraft altitude. A fixed

20   global a priori profile x_a is used for all the retrievals, shown in the top left panel of Fig. 1. Its variability is given in the top middle panel, calculated from the square root of the diagonal of the a priori covariance matrix, given in the upper right panel. We see the highest variability in the lowermost layers of the atmosphere, due to localised fossil fuel and biomass burning, with an a priori variability of ∼70 % at the surface

25   decreasing to 50 % near 800 hPa (∼1.5 km) and to 20–30 % for pressures lower than 600 hPa (∼4 km).

In this spectral range, H_2O is the main interfering gas, while N_2O contributes to the signal at higher wavenumbers. To account for their contributions, both profiles are retrieved simultaneously with CO, as well as surface temperature.

Retrieval of MetOp-A/IASI CO profiles and validation

E. De Wachter et al.

Title Page

Abstract	Introduction
Conclusions	References
Tables	Figures

|◄ | ►|
| ◄ | ► |

Back | Close

Full Screen / Esc

Printer-friendly Version

Interactive Discussion

A cloud filtering is applied according to Clerbaux et al. (2009), based on the AVHRR-derived fractional cloud cover from the IASI EUMETSAT L2 products. Only pixels with a cloud fraction between 0 and 25 % are processed. In addition, the brightness temperature at the 11 µm (BT11) and 12 µm (BT12) IASI channels are compared to the ECWMF skin temperature. If either the difference between BT12 and the ECMWF skin temperature is larger than 10 K or if BT11 and BT12 are differing more than ±10 K, the pixel is considered as contaminated and eliminated.

2.3 FORLI

The FORLI algorithm has been developed at the Université Libre de Bruxelles (ULB). It uses pre-calculated look-up tables of absorbance cross sections at various pressures and temperatures instead of the more time consuming line-by-bine calculations, and the optimal estimation for the inverse scheme (Hurtmans et al., 2012). CO profiles are calculated on 19 fixed layers from the surface up to the top of the atmosphere (set to 60 km), corresponding to 18 equidistant layers of 1 km from 0 km to 18 km, and a top layer between 18 and 60 km.

FORLI CO profiles are retrieved from radiances in the spectral range 2143–2181 cm^{-1} (same interval as SOFRID). A diagonal measurement error covariance matrix was chosen, with an average measurement noise corresponding to 1.8×10^{-9} W(cm^2 sr cm^{-1})$^{-1}$, the estimated radiometric noise in this spectral region (Clerbaux et al., 2009). The operational MetOp-A L2 temperature and humidity profiles are used for the radiative transfer calculations. To take into account the wavenumber dependency of the surface emissivity, a climatology built from several years of IASI data (Zhou et al., 2011) is used. In the few cases there are missing values in the Zhou et al. (2011) climatology, the MODIS/TERRA climatology (Wan, 2008) is used instead.

The a priori information was constructed from aircraft profiles from the MOZAIC program, complemented by ACE-FTS (Clerbaux et al., 2005) profiles at the highest altitudes (upper troposphere and above), as well as distributions from the LMDz-INCA (Hauglustaine et al., 2004) global chemistry transport model. The bottom panels of

Fig. 1 display the a priori profile, its associated variability and covariance matrix. Compared to SOFRID we see smaller volume mixing ratios (vmrs) near the surface for the a priori profile, and a steeper descending profile in the upper troposphere. FORLI presents larger a priori variability in the upper troposphere (∼35 %) and in the UTLS (∼45 %). Surface temperature, CO_2 and N_2O total columns, and a H_2O profile are retrieved in addition to the CO profile.

For profiles in the Arctic, Pommier et al. (2010) found differences between FORLI CO and smoothed in situ profiles lower than 17 % in spring, and stated that FORLI overestimates the CO concentrations compared to the in situ data in summer where differences can reach up to 20 % below 8 km for polluted cases. George et al. (2009) found total column discrepancies of about 7 % between IASI and the other sounders (for the NH and equatorial region), going up to 17 % when high CO concentrations are found e.g. during fire events.

The FORLI CO products are publicly available via the Ether (http://ether.ipsl.jussieu.fr/) database. The data is updated every day with a delay of one month and includes the twice daily distributions of CO total columns since October 2007 along with averaging kernels, associated errors, and quality flags.

For the comparison with MOZAIC data, only the more reliable pixels were taken into account using the quality flags (super quality flag equal to 0). For more information see http://ether.ipsl.jussieu.fr/ether/pubipsl/iasi_CO_uk.jsp.

3 MOZAIC

The MOZAIC program provides routine measurements of reactive gases on long distance commercial aircraft (Marenco et al., 1998). Since 1994, five airliners have been equipped with O_3 and relative humidity instruments, and a CO analyser was successfully added in December 2001. One aircraft carries an additional instrument to measure total odd nitrogen (NO_y) since 2001 (Volz-Thomas et al., 2005). With a measurement precision of ±5 ppbv for a 30 s integration time, the CO analyser has a

horizontal resolution of about 7 km and a vertical resolution of about 300 m during ascents and descents (Nedelec et al., 2003). The MOZAIC data is freely accessible for scientific use at http://www.iagos.org. Since 2009, the MOZAIC program has been expanded, implementing other commercial in-service aircraft observation programs such as CARIBIC (http://www.caribic-atmospheric.com) into the IAGOS Research Infrastructure (In-service Aircraft for a Global Observing System). In the following however, for simplicity, we will continue to refer to the MOZAIC data.

For the validation of IASI CO, MOZAIC aircraft observations during take-off and landing were taken for the 2008–2009 period. In addition, we will investigate the temporal behavior of the data recorded from flights between Frankfurt, Germany (50.1° N, 8.7° E) and Windhoek, Namibia (22.6° S, 17.1° E). These flights are strongly represented in the dataset and can give us insight in any latitudinal dependency of the quality of the two IASI products.

4 Validation

4.1 Methodology and information content

Pixels were selected within ±1° in latitude and longitude from the MOZAIC coordinates. The quality assessment is based on the comparison of partial columns and a distinction is made between daytime and nighttime IASI retrievals. The averaging kernel matrix **A** is an important by-product of the retrieval, which characterizes the sensitivity of the retrieved profile to the true profile. The rows of **A** are called the averaging kernels and are peaked functions. For each retrieval level, the width of the averaging kernels corresponds to the altitude range contributing to the retrieved value and therefore gives an indication of the height resolution. The DFS (Degrees of Freedom for Signal) is calculated from the trace of **A** and quantifies the number of independent pieces of information on the vertical for each measurement. Calculation of the DFS, for all coincidences with MOZAIC data, gives values which vary between 1.4 and 2.3 for SOFRID

Retrieval of MetOp-A/IASI CO profiles and validation

E. De Wachter et al.

and between 1.1 and 2.1 for FORLI. This shows that nearly 2 independent pieces of information can be deduced from the retrieved SOFRID and FORLI CO profiles in the best cases.

Daytime and nighttime averaging kernels of SOFRID and FORLI are shown for Frankfurt (Fig. 2) and Windhoek (Fig. 3). Based on the forms and peaks of the averaging kernels, a lower (surface-480 hPa) and upper (480–225 hPa) tropospheric partial columns were defined. The upper limit of 225 hPa was chosen to be within the boundary level of the aircraft profiles. The partial column averaging kernels for the lower and upper troposphere are given in black and were calculated according to Deeter (2002). At the two locations, we see differences between daytime and nighttime partial column averaging kernels: for nighttime measurements the vertical resolution (width of the averaging kernels) is lower and the maximum sensitivity is shifted upwards for the lower tropospheric averaging kernels. Especially at Frankfurt, FORLI daytime and nighttime averaging kernels show strong differences. The sensitivity near the surface is higher during the day. The lower and upper tropospheric nighttime averaging kernels are strongly overlapping, meaning that the lower and upper tropospheric information is correlated. For SOFRID the differences between daytime and nighttime averaging kernels are smaller. At both locations, the maximum sensitivity of the nighttime averaging kernels in the upper troposphere is shifted towards lower altitudes. The SOFRID lower tropospheric nighttime averaging kernel at Windhoek shows an irregularity in the upper troposphere.

4.2 Global comparisons

Global maps of lower (surface-480 hPa) and upper (480–225 hPa) tropospheric CO columns retrieved with SOFRID and FORLI are displayed in Fig. 4. Daily means are shown for 1 January and 1 July 2008, characterizing the winter and summer seasons.

In general the same features are captured by the two algorithms. The four top figures provide a boreal winter picture, with elevated CO values in the lower troposphere over West Africa, where biomass burning fires are active from October through January

Title Page

Abstract | Introduction

Conclusions | References

Tables | Figures

◄ | ►►

◄ | ►

Back | Close

Full Screen / Esc

Printer-friendly Version

Interactive Discussion

in the Sahel region. This CO-rich air is convectively uplifted to the upper troposphere where it disperses over the African tropics towards the east coast of South America and the South Arabian peninsula (Edwards et al., 2003). In the lower troposphere, higher CO concentrations are found by FORLI compared to SOFRID for these regions affected by biomass burning. Over South-East Asia, IASI detects highly polluted air-masses that are uplifted and advected along the North-East Asian coast. In these pollution cases higher CO columns are retrieved by FORLI than by SOFRID. In the upper troposphere, higher CO background values are observed by SOFRID at midlatitudes.

In the bottom four figures, visualising the CO distributions on 1 July 2008, we see a shift of the biomass burning region from West Africa to Central Africa, featuring the beginning of the vegetation burning season, which lasts up to November. Both algorithms capture the displacement of a large plume of polluted air originating from North-East Asia which is rapidly transported over the Northern Pacific towards the Western Canadian coast. FORLI shows a band of elevated lower tropospheric CO values over Northern Europe and North Russia, which is not observed by SOFRID. Similar signatures are found on 1 January 2008. Again, higher upper tropospheric CO background values are observed by SOFRID at midlatitudes.

In conclusion, SOFRID and FORLI show similar global distributions. FORLI retrieves higher CO concentrations in the lower troposphere for regions affected by biomass or fossil fuel burning, and lower CO background values in the midlatitudinal upper troposphere, compared to SOFRID.

4.3 Correlations

Table 1 presents the results of a linear regression analysis between the two IASI retrieval products and MOZAIC partial columns for 980 coincident observations in 2008 and 2009. To account for the different resolution between the satellite and high resolution in-situ data, a smoothing was applied to the MOZAIC profiles x_{MOZ} by the IASI averaging kernels:

$$\hat{x}_{MOZ} = x_a + \mathbf{A} \cdot (x_{MOZ} - x_a) \tag{1}$$

where $\hat{x}_{MOZ}$ is the smoothed or convolved MOZAIC profile and x_a and $\mathbf{A}$ are the a priori profile and averaging kernel matrix of the IASI retrieval (SOFRID or FORLI).

Table 1 gives the slope (a), intercept (b) and correlation coefficient (r) of the compari-
son of IASI partial columns with *smoothed* MOZAIC partial columns. In brackets results of the comparison with partial columns calculated from the *raw* MOZAIC profiles are given. As expected, we see an improvement after smoothing of the in-situ data with the IASI averaging kernels. A high correlation is found in the lower troposphere (surface-480 hPa), with $r \sim 0.8$ for both retrievals. In the upper troposphere (480–225 hPa) the correlation coefficients are $\sim$0.7. For both algorithms, we see a slight improvement for daytime compared to nighttime retrievals. Excellent agreement is found between day-time FORLI and smoothed MOZAIC lower tropospheric columns showing a slope of 1 and an intercept near 0. Daytime lower tropospheric SOFRID and smoothed MOZAIC are in good agreement with a slope of 0.76 and intercept of 0.32.

Better insight on the quality of the satellite data is gained by analysing the temporal variations of CO.

4.4 Temporal variation

Figures 5 and 6 present time series of lower and upper tropospheric columns at the airports of Frankfurt and Windhoek, respectively. Blue lines represent the relative dif-ference between smoothed MOZAIC and IASI partial columns, and the mean (μ) and standard deviation (σ) are displayed in the figures. The retrieval error presented (pink bars and contours) is the sum of the smoothing error and the measurement error. The smoothing error is the dominant source of error for CO retrievals in the TIR (Barret et al., 2005) and accounts for the low vertical resolution of the retrievals. SOFRID provides a mean retrieval error of 16.1 % (17.5 %) for the surface-480 hPa partial column and of 8.5 % (6.5 %) for the 480–225 hPa partial column at Frankfurt (Windhoek). FORLI

mean errors at Frankfurt (Windhoek) range from 13.5 % (16.5 %) in the lower to 6.6 % (7.2 %) in the upper troposphere. The retrieval errors computed by both algorithms are therefore in good agreement.

At Frankfurt (Fig. 5), both products capture the same seasonal variability as the aircraft observations, but underestimate the maxima in winter-spring in the lower troposphere. However, we see a great improvement after smoothing of the MOZAIC data, clearly visible for the 2009 winter-spring period. This may be linked to the insensitivity of IASI to boundary layer (BL) pollution in winter-spring when the BL height is low. A comparison between IASI and MOZAIC profiles will allow us to better understand these discrepancies (see the discussion below on Figs. 7 and 8). Lower tropospheric columns of SOFRID and smoothed MOZAIC are in very good agreement, with exception of the small positive bias in July–October 2008, leading to a mean relative difference with smoothed MOZAIC of −3.6 %. Note the excellent agreement in terms of small-scale variability from January to September 2009. FORLI overestimates the lower tropospheric CO concentration relative to smoothed MOZAIC with a mean positive bias of 13.0 %. Furthermore, differences larger than 30 % occur throughout the studied period. In the upper troposphere, FORLI and smoothed MOZAIC are in close agreement, with alternating slightly higher and lower CO concentrations, leading to a mean relative difference of 0.9 %. SOFRID underestimates the seasonal variability in the upper troposphere and shows overall a positive bias of 10.5 % relative to MOZAIC. The standard deviation of the relative difference between retrieved and smoothed partial columns (σ) is comparable for the lower and upper troposphere and is ∼14 % and ∼16–17 % for SOFRID and FORLI, respectively. With exception of the lower tropospheric value of 14.3 % for SOFRID, these values are higher than the retrieval errors estimated (pink contours), especially in the upper troposphere.

At Windhoek (Fig. 6), for both algorithms, we see a very good reproduction of the variability resulting from the vegetation fires in Southern Africa from August to November. In the lower troposphere, excellent agreement is found between SOFRID and smoothed MOZAIC for the fire emission peaks, but we see an overestimation of the

Retrieval of MetOp-A/IASI CO profiles and validation

E. De Wachter et al.

background CO values in December–July, leading to a mean relative difference of −12.8 %. Lower tropospheric FORLI and smoothed MOZAIC are in excellent agreement over the whole period with a mean relative difference of −1.6 %, although slightly higher values for the fire maxima are observed by FORLI relative to smoothed MOZAIC (~10 %).

In the upper troposphere, FORLI is biased low relative to both raw and smoothed MOZAIC, most pronounced in 2008, giving a mean relative difference of 10.2 %. Upper tropospheric SOFRID and smoothed MOZAIC are in very good agreement (−3.7 %). Note the great improvement after smoothing for the third fire maxima in October 2008, where SOFRID overestimates the CO concentration compared to raw MOZAIC (the same holds for FORLI as well, if one would correct for the bias). In this case, a possible cause could be the contamination of upper tropospheric CO with lower tropospheric CO. As can be seen from Fig. 3, the averaging kernel of the upper tropospheric partial column (dashed black line) shows sensitivity to the lower troposphere. The extreme CO values found during the vegetation fire season, in combination with the high extension of the fire plumes (see discussion below) lead to this contamination effect. However, strong differences between the raw and smoothed MOZAIC data seem to be limited to this specific period.

In order to produce a complete picture of the performance of both retrievals, time series and mean differences of MOZAIC and IASI CO profiles at Frankfurt and Windhoek are displayed in Figs. 7 and 8. IASI daytime and nighttime comparisons with raw and smoothed MOZAIC profiles are shown. It is worth noting that Figs. 7 and 8 clearly highlight the different pollution conditions we have at the two airports; Frankfurt, a region affected by BL pollution (typically below 800 hPa), and Windhoek, a region affected by biomass fire plumes in Southern Africa, which are injected to higher altitudes (up to ~500 hPa; Rio et al., 2010).

At Frankfurt (Fig. 7), we see a confirmation of the earlier assumption that the high CO concentrations observed by MOZAIC correspond to local CO emissions only affecting the BL. This pollution is not detected by the IASI instrument in winter when thermal

Title Page

Abstract | Introduction

Conclusions | References

Tables | Figures

◄ | ►|

◄ | ►

Back | Close

Full Screen / Esc

Printer-friendly Version

Interactive Discussion

contrast and the BL are low, leading to relative differences between raw MOZAIC and SOFRID profiles up to 40 % at the surface. After smoothing we see a much better agreement in the lower troposphere, with relative differences between smoothed MOZAIC and daytime SOFRID profiles of less than −3 %. SOFRID nighttime retrievals underestimate the BL pollution and slightly overestimate the CO background concentrations leading to differences with smoothed MOZAIC ranging from +13 % at the surface to −7.5 % at 400 hPa. In the upper troposphere, SOFRID shows a rather flat distribution with a positive bias, as previously seen in Fig. 6.

FORLI retrieves well the BL pollution compared to raw MOZAIC, with exception of the winter period due to the earlier explained limited sensitivity of IASI. Also, elevated CO values are retrieved by FORLI in July–August 2008 (most pronounced in the nighttime set), which are not observed in the raw MOZAIC data. The smoothed MOZAIC profiles demonstrate that the FORLI vertical resolution results in a diffusion of the raw MOZAIC BL CO concentrations to higher altitudes and leads to differences ranging from more than −20 % at the surface to 0 % at 510 hPa between smoothed MOZAIC and FORLI daytime profiles (around −15 % in the free troposphere for nighttime retrievals).

At Frankfurt, FORLI nighttime profiles are more smoothed over the lower troposphere than daytime retrievals. This difference results from the lower resolution for nighttime retrievals, as evidenced with Fig. 2 in Sect. 4.1.

At Windhoek, we can deduce from the raw MOZAIC profiles (Fig. 8 upper panels) that the CO emitted by the vegetation fires in Southern Africa mostly impacts the troposphere up to 400 hPa. During the fire periods, IASI retrieved profiles and MOZAIC smoothed profiles show high CO concentrations up to 225 hPa indicating a contamination by the fire emissions above 400 hPa.

Nighttime SOFRID retrievals underestimate the high CO concentrations in the low and free troposphere during the vegetation fire period and overestimate the low CO background values, leading to the overall positive bias estimated by the relative differences. The same kind of behaviour was found at Frankfurt indicating a smoothing of the extreme CO values by SOFRID nighttime retrievals larger than

indicated by the MOZAIC smoothed data. The radiometric noise set conservatively to $1.41 \times 10^{-8}\,\mathrm{W\,(cm^2\,sr\,cm^{-1})^{-1}}$ may be too high resulting in a reduced retrieved variability.

The negative bias of 10.0 % previously identified for FORLI in the upper troposphere (Fig. 6), is seen here by the underestimation of the CO concentrations above 480 hPa compared to MOZAIC. This bias is more pronounced for the daytime compared to nighttime retrievals.

5 Conclusions

This study presented tropospheric CO profiles retrieved from IASI spectra by two different retrieval algorithms, SOFRID and FORLI. A quality assessment of the retrieved IASI CO products was given by a detailed comparison with airborne observations from the MOZAIC program, for the years 2008–2009. A correlation study of the coincidences between MOZAIC and the two IASI products of lower (surface-480 hPa) and upper (480–225 hPa) tropospheric partial columns showed a very good (resp. good) agreement for lower (resp. upper) tropospheric columns, with correlation coefficients $r \sim 0.8$ (resp. $r \sim 0.7$). In the lower troposphere, FORLI reproduced the amplitude of the variations of smoothed MOZAIC data better than SOFRID (slopes closer to 1). The variability of the MOZAIC smoothed data was slightly better captured by SOFRID, showing higher correlation coefficients.

The temporal variation of lower and upper tropospheric columns, as well as daytime and nighttime CO profiles, was investigated in detail at the two airports Frankfurt and Windhoek. On the overall, both retrieval products showed a good agreement with smoothed MOZAIC partial columns in terms of seasonal variability, and especially in the lower troposphere. At Frankfurt, the pronounced smoothing of the MOZAIC profiles by the averaging kernels of SOFRID and FORLI in the winter-spring period, indicated the insensitivity of IASI to BL pollution when thermal contrast is low.

SOFRID partial columns were found to be in very good agreement with smoothed MOZAIC in the lower troposphere (−3.8 % at Frankfurt), with exception of the overestimation of the low CO background values (12.8 %) at Windhoek. In the upper troposphere, SOFRID was biased high (10.5 %) at Frankfurt but showed a very good agreement with smoothed MOZAIC at Windhoek (−3.7 %). Profile comparisons demonstrated an overestimation of CO background values and an underestimation of the high CO values by the nighttime SOFRID retrievals.

FORLI lower tropospheric columns were positively biased (13.0 %) at Frankfurt. A closer investigation of the profiles revealed that the nighttime retrievals could not inform on the polluted boundary layer concentrations. At Windhoek, we found a very good agreement between FORLI and smoothed MOZAIC, with only slightly higher values for the fire maxima (~10 %). In the upper troposphere, FORLI showed a very good agreement with MOZAIC at Frankfurt (0.9 %) and was biased low at Windhoek (10.0 %). Daytime and nighttime profiles at Windhoek of both SOFRID and FORLI indicated signatures of lower tropospheric contamination in the upper troposphere.

In conclusion, SOFRID and FORLI demonstrated to be in good agreement with the MOZAIC reference set and showed their ability to correctly reproduce the CO variability in the lower and upper troposphere. Discrepancies found between the two IASI products and MOZAIC could mostly be traced back to a reduced performance of the nighttime retrievals, which is related to the lower thermal contrast during nighttime compared to daytime, which leads to less vertically resolved nighttime measurements.

The publication of this article is financed by CNRS-INSU.

References

Barret, B., Turquety, S., Hurtmans, D., Clerbaux, C., Hadji-Lazaro, J., Bey, I., Auvray, M., and Coheur, P.-F.: Global carbon monoxide vertical distributions from spaceborne high-resolution FTIR nadir measurements, Atmos. Chem. Phys., 5, 2901–2914, doi:10.5194/acp-5-2901-2005, 2005. 3282

Barret, B., Le Flochmoën, E., Sauvage, B., Pavelin, E., Matricardi, M., and Cammas, J. P.: The detection of post-monsoon tropospheric ozone variability over south Asia using IASI data, Atmos. Chem. Phys., 11, 9533–9548, doi:10.5194/acp-11-9533-2011, 2011. 3273, 3275

Bergamaschi, P., Hein, R., Heimann, M., and Crutzen, P. J.: Inverse modeling of the global CO cycle 1. Inversion of CO mixing ratios, J. Geophys. Res., 105, 1909–1927, 2000. 3273

Borbas, E. E. and Ruston, B. C.: The RTTOV UWiremis IR land surface emissivity module, Associate Scientist mission report, Mission no. AS09-04, Document NWPSAF-MO-VS-042, Version 1.0, EUMETSAT Numerical Weather Prediction Satellite Applications Facility, Met Office, Exeter, UK, June 2010. 3276

Title Page

Abstract | Introduction

Conclusions | References

Tables | Figures

◀ | ▶

◀ | ▶

Back | Close

Full Screen / Esc

Printer-friendly Version

Interactive Discussion

Brenninkmeijer, C. A. M. and Novelli, P. C.: Carbon monoxide, in: Encyclopedia Atmospheric Sciences, edited by: Holton, J. R., Academic Press, an imprint of Elsevier Science, London, 2389–2396, 2003. 3272, 3273

Chin, M., Jacob., D. J., Munger, J. W., Parrish, D. D., and Doddridge, B. G.: Relationship of ozone and carbon monoxide over North America, J. Geophys. Res., 99, 565–573, 1994. 3273

Clerbaux, C., Coheur, P.-F., Hurtmans, D., Barret, B., Carleer, M., Colin, R., Semeniuk, K., McConnell, J. C., Boone, C., and Bernath, P.: Carbon monoxide distribution from the ACE-FTS solar occultation measurements, Geophys. Res. Lett., 32, L16S01, doi:10.1029/2005GL022394, 2005. 3277

Clerbaux, C., Boynard, A., Clarisse, L., George, M., Hadji-Lazaro, J., Herbin, H., Hurtmans, D., Pommier, M., Razavi, A., Turquety, S., Wespes, C., and Coheur, P.-F.: Monitoring of atmospheric composition using the thermal infrared IASI/MetOp sounder, Atmos. Chem. Phys., 9, 6041–6054, doi:10.5194/acp-9-6041-2009, 2009. 3273, 3275, 3277

Clough, S. A., Shephard, M. W., Mlawer, E. J., Delamere, J. S., Iacono, M. J., Cady-Pereira, K., Boukabara, S., and Brown, P. D.: Atmospheric radiative transfer modeling: a summary of the AER codes, J. Quant. Spectrosc. Ra., 91, 233–244, 2005. 3276

Deeter, M.: Calculation and application of MOPITT averaging kernels, available at: http://www.acd.ucar.edu/mopitt/data-interpretation.shtml, last access: 24 July 2002. 3280

Dufour, G., Eremenko, M., Griesfeller, A., Barret, B., LeFlochmoën, E., Clerbaux, C., Hadji-Lazaro, J., Coheur, P.-F., and Hurtmans, D.: Validation of three different scientific ozone products retrieved from IASI spectra using ozonesondes, Atmos. Meas. Tech., 5, 611–630, doi:10.5194/amt-5-611-2012, 2012. 3275

Edwards, D. P., Lamarque, J.-F., Attié, J.-L., Emmons, L. K., Richter, A., Cammas, J.-P., Gille, J. C., Francis, G. L., Deeter, M. N., Warner, J., Ziskin, D. C., Lyjak, L. V., Drummond, J. R., and Burrows, J. P.: Tropospheric ozone over the Tropical Atlantic: a satellite perspective, J. Geophys. Res., 108, 4237, doi:10.1029/2002JD002927, 2003. 3281

Forster, C., Wandinger, W., Wotawa, G., James, P., Mattis, I., Althausen, D., Simmonds, P., O'Doherty, S., Jennings, S. G., Kleefeld, C., Schneider, J., Trickl, T., Kreipl, S., Jäger, H., and Stohl, A.: Transport of boreal forest fire emissions from Canada to Europe, J. Geophys. Res., 106, 887–906, 2001. 3273

George, M., Clerbaux, C., Hurtmans, D., Turquety, S., Coheur, P.-F., Pommier, M., Hadji-Lazaro, J., Edwards, D. P., Worden, H., Luo, M., Rinsland, C., and McMillan, W.: Carbon

Retrieval of MetOp-A/IASI CO profiles and validation

E. De Wachter et al.

Title Page

Abstract | Introduction

Conclusions | References

Tables | Figures

◄ | ►

◄ | ►

Back | Close

Full Screen / Esc

Printer-friendly Version

Interactive Discussion

monoxide distributions from the IASI/METOP mission: evaluation with other space-borne remote sensors, Atmos. Chem. Phys., 9, 8317–8330, doi:10.5194/acp-9-8317-2009, 2009. 3274, 3278

Hauglustaine, D. A., Hourdin, F., Jourdain, L., Filiberti, M.-A., Walters, S., Lamarque, J.-F., and Holland, E. A.: Interactive chemistry in the Laboratoire de Météorologie Dynamique general circulation model: description and background tropospheric chemistry, J. Geophys. Res., 109, D04314, doi:10.1029/2003JD003957, 2004. 3277

Hurtmans, D., Coheur, P. F., Wespes, C., Clarisse, L., Scharf, O., Clerbaux, C., Hadji-Lazaro, J., George, M., and Turquety, S.: FORLI radiative transfer and retrieval code for IASI, J. Quant. Spectrosc. Ra., doi:10.1016/j.jqsrt.2012.02.036, in press, 2012. 3274, 3277

Logan, J., Prather, M. J., Wofsy, S. C., and McElroy, M. B.: Tropospheric chemistry: a global perspective, J. Geophys. Res., 86, 7210–7254, 1981. 3273

Marenco, A., Thouret, V., Nédélec, P., Smit, H., Helten, M., Kley, D., Karcher, F., Simon, P., Law, K., Pyle, J., Poschmann, G., Von Wrede, R., Hume, C., and Cook, T.: Measurement of ozone and water vapour by Airbus in-service aircraft: the MOZAIC airborne program, An overview, J. Geophys. Res., 103, 25631–25642, 1998. 3273, 3278

Matricardi, M.: Technical Note: An assessment of the accuracy of the RTTOV fast radiative transfer model using IASI data, Atmos. Chem. Phys., 9, 6899–6913, doi:10.5194/acp-9-6899-2009, 2009. 3275

Matricardi, M., Chevallier, F., Kelly, G., and Thepaut, J. N.: An improved general fast radiative transfer model for the assimilation of radiance observations, Q. J. Roy. Meteorol. Soc., 130, 153–173, 2004. 3275, 3276

Nedelec, P., Cammas, J.-P., Thouret, V., Athier, G., Cousin, J.-M., Legrand, C., Abonnel, C., Lecoeur, F., Cayez, G., and Marizy, C.: An improved infrared carbon monoxide analyser for routine measurements aboard commercial Airbus aircraft: technical validation and first scientific results of the MOZAIC III programme, Atmos. Chem. Phys., 3, 1551–1564, doi:10.5194/acp-3-1551-2003, 2003. 3279

Parrish, D. D., Holloway, J. S., Trainer, M., Murphy, P. C., Forbes, G. L., and Fehsenfeld, F. C.: Export of North American ozone pollution to the North Atlantic Ocean, Science, 259, 1436–1439, 1993. 3273

Pavelin, E. G., English, S. J., and Eyre, J. R.: The assimilation of cloud-affected infrared satellite radiances for numerical weather prediction, Q. J. Roy. Meteorol. Soc., 134, 737–749, 2008. 3275

Retrieval of MetOp-A/IASI CO profiles and validation

E. De Wachter et al.

Title Page

Abstract	Introduction
Conclusions	References
Tables	Figures

◄◄   ►►

◄   ►

Back   Close

Full Screen / Esc

Printer-friendly Version

Interactive Discussion

Pommier, M., Law, K. S., Clerbaux, C., Turquety, S., Hurtmans, D., Hadji-Lazaro, J., Coheur, P.-F., Schlager, H., Ancellet, G., Paris, J.-D., Nédélec, P., Diskin, G. S., Podolske, J. R., Holloway, J. S., and Bernath, P.: IASI carbon monoxide validation over the Arctic during POLARCAT spring and summer campaigns, Atmos. Chem. Phys., 10, 10655–10678, doi:10.5194/acp-10-10655-2010, 2010. 3274, 3278

Rio, C., Hourdin, F., and Chédin, A.: Numerical simulation of tropospheric injection of biomass burning products by pyro-thermal plumes, Atmos. Chem. Phys., 10, 3463–3478, doi:10.5194/acp-10-3463-2010, 2010. 3284

Rodgers, C. D.: Inverse Methods for Atmospheric Sounding: Theory and Practice, World Scientific Publishing Co. Pte. Ltd., Singapore, 2000. 3275

Rothman, L. S., Jacquemart, D., Barbe, A., Benner, D. C., Birk, M., Brown, L. R., Carleer, M. R., Chackerian Jr., C., Chance, K., Coudert, L. H., Dana, V., Devi, V. M., Flaud, J.-M., Gamache, R. R., Goldman, A., Hartmann, J.-M., Jucks, K. W., Maki, A. G., Mandin, J.-Y., Massie, S. T., Orphal, J., Perrin, A., Rinsland, C. P., Smith, M. A. H., Tennyson, J., Tolchenov, R. N., Toth, R. A., Vander Auwera, J., Varanasi, P., and Wagner, G.: The HITRAN 2004 molecular spectroscopic database, J. Quant. Spectrosc. Ra., 96, 139–204, 2005. 3276

Saunders, R., Matricardi, M., and Brunel, P.: An improved fast radiative transfer model for assimilation of satellite radiance observations, Q. J. Roy. Meteorol. Soc. B, 125, 1407–1425, 1999. 3275

Schlüssel, P., Hultberg, T. H., Phillips, P. L., August, T., and Calbet, X.: The operational IASI Level 2 processor, Adv. Space Res., 36, 982–988, doi:10.1016/j.asr.2005.03.008, 2005. 3276

Turquety, S., Hurtmans, D., Hadji-Lazaro, J., Coheur, P.-F., Clerbaux, C., Josset, D., and Tsamalis, C.: Tracking the emission and transport of pollution from wildfires using the IASI CO retrievals: analysis of the summer 2007 Greek fires, Atmos. Chem. Phys., 9, 4897–4913, doi:10.5194/acp-9-4897-2009, 2009. 3274

Volz-Thomas, A., Berg, M., Heil, T., Houben, N., Lerner, A., Petrick, W., Raak, D., and Pätz, H.-W.: Measurements of total odd nitrogen (NO_y) aboard MOZAIC in-service aircraft: instrument design, operation and performance, Atmos. Chem. Phys., 5, 583–595, doi:10.5194/acp-5-583-2005, 2005. 3278

Title Page

Abstract | Introduction

Conclusions | References

Tables | Figures

◀ | ▶

◀ | ▶

Back | Close

Full Screen / Esc

Printer-friendly Version

Interactive Discussion

Voulgarakis, A., Telford, P. J., Aghedo, A. M., Braesicke, P., Faluvegi, G., Abraham, N. L., Bowman, K. W., Pyle, J. A., and Shindell, D. T.: Global multi-year O_3-CO correlation patterns from models and TES satellite observations, Atmos. Chem. Phys., 11, 5819–5838, doi:10.5194/acp-11-5819-2011, 2011. 3273

5   Wan, Z.: New refinements and validation of the MODIS Land-Surface Temperature/Emissivity products, Remote Sens. Environ., 112, 59–74, doi:10.1016/j.rse.2006.06.026, 2008. 3277

Zhou, D. K., Larar, A. M., Liu, X., Smith, W. L., Strow, L. L., and Yang, P.: Global land surface emissivity retrieved from satellite ultraspectral IR measurements, IEEE T. Geosci. Remote, 49, 1277–1290, doi:10.1109/TGRS.2010.2051036, 2011. 3277

Title Page

Abstract | Introduction

Conclusions | References

Tables | Figures

◄ | ►

◄ | ►

Back | Close

Full Screen / Esc

Printer-friendly Version

Interactive Discussion

Table 1. Slope (*a*), intercept (*b*) and correlation coefficients (*r*) of the linear least squares fit of CO partial columns computed from MOZAIC profiles and IASI retrieved profiles (SOFRID – top, FORLI – bottom). Results are given for lower (surface-480 hPa) and upper (480–225 hPa) tropospheric partial columns of raw (brackets) and smoothed MOZAIC compared to daytime and nighttime IASI retrievals.

		a		*b*		*r*	
		SOFRID					
surface-480 hPa	day	(0.52)	0.76	(0.52)	0.32	(0.69)	0.85
	night	(0.42)	0.57	(0.66)	0.53	(0.70)	0.80
480–225 hPa	day	(0.37)	0.51	(0.30)	0.24	(0.58)	0.70
	night	(0.30)	0.43	(0.35)	0.29	(0.50)	0.62
		FORLI					
surface-480 hPa	day	(0.64)	1.01	(0.47)	0.09	(0.63)	0.79
	night	(0.54)	0.84	(0.59)	0.30	(0.65)	0.74
480–225 hPa	day	(0.30)	0.57	(0.25)	0.14	(0.42)	0.71
	night	(0.31)	0.59	(0.27)	0.17	(0.42)	0.65
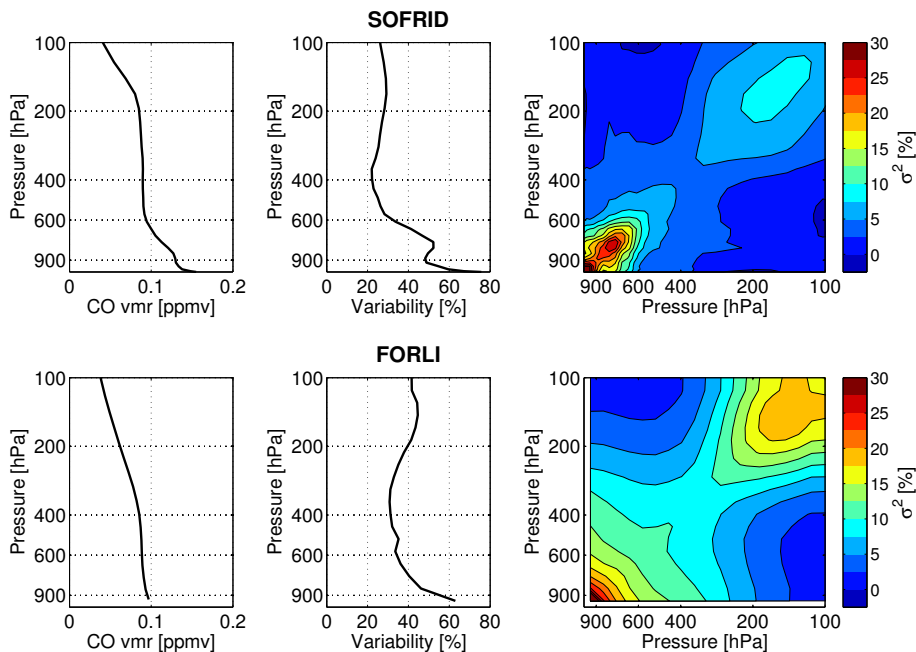
Fig. 1. For SOFRID (top panels) and FORLI (bottom panels): the a priori profile (left panel), the a priori variability (middle panel) and the a priori covariance matrix (right panel).
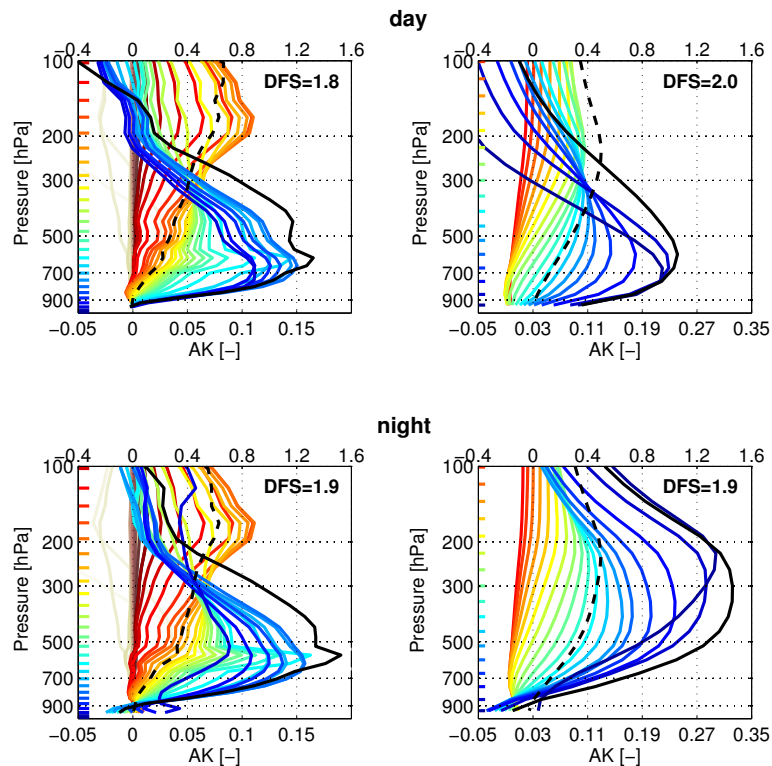
Fig. 2. SOFRID (left panel) and FORLI (right panel) averaging kernels (AK) (bottom x-axis, color lines) and normalised averaging kernels of partial columns (top x-axis, black solid line– surface-480 hPa – and black dashed line – 480–225 hPa), for a daytime (top panels) and nighttime (bottom panels) retrieval of a IASI pixel near Frankfurt (50.1° N, 8.7° E) on 28 May 2008. The nominal height of each averaging kernel is marked by the horizontal tick with corresponding colour.
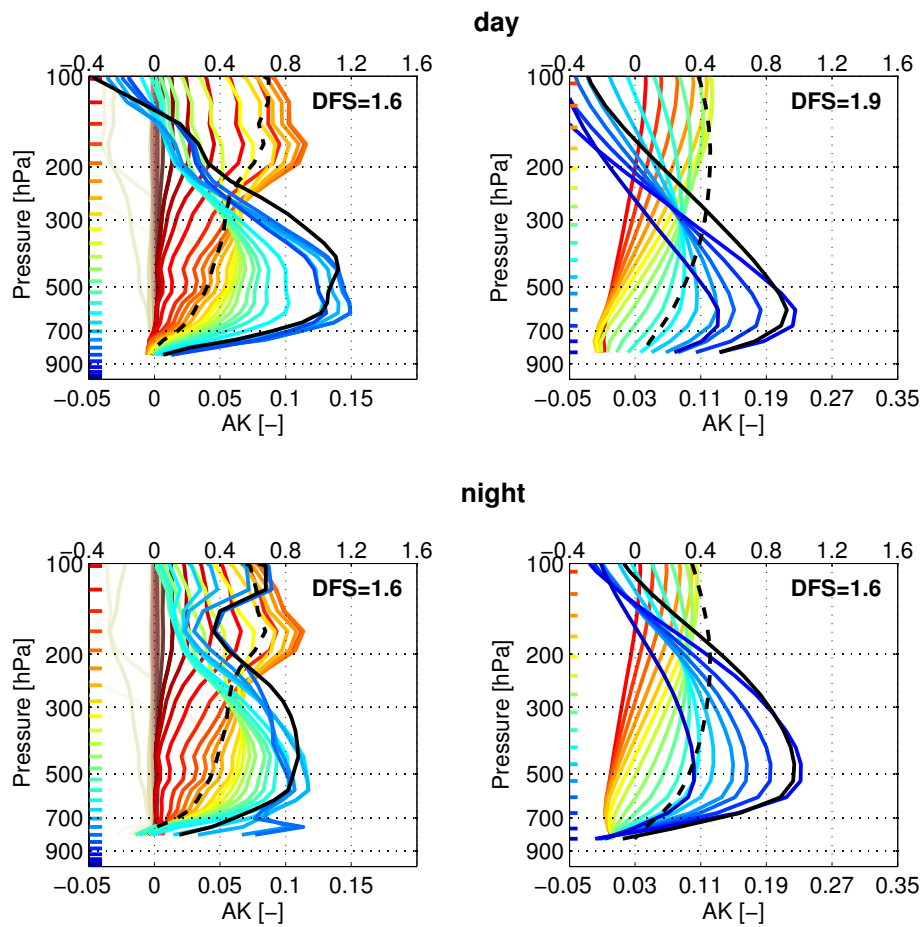
Fig. 3. As Fig. 2 for Windhoek (22.6° S, 17.1° E) on 24 January 2008. Windhoek lies at an altitude ~1700 m hence the lower cut-off of the averaging kernels.

Title Page

Abstract | Introduction

Conclusions | References

Tables | Figures

|◄ | ►|

◄ | ►

Back | Close

Full Screen / Esc

Printer-friendly Version

Interactive Discussion
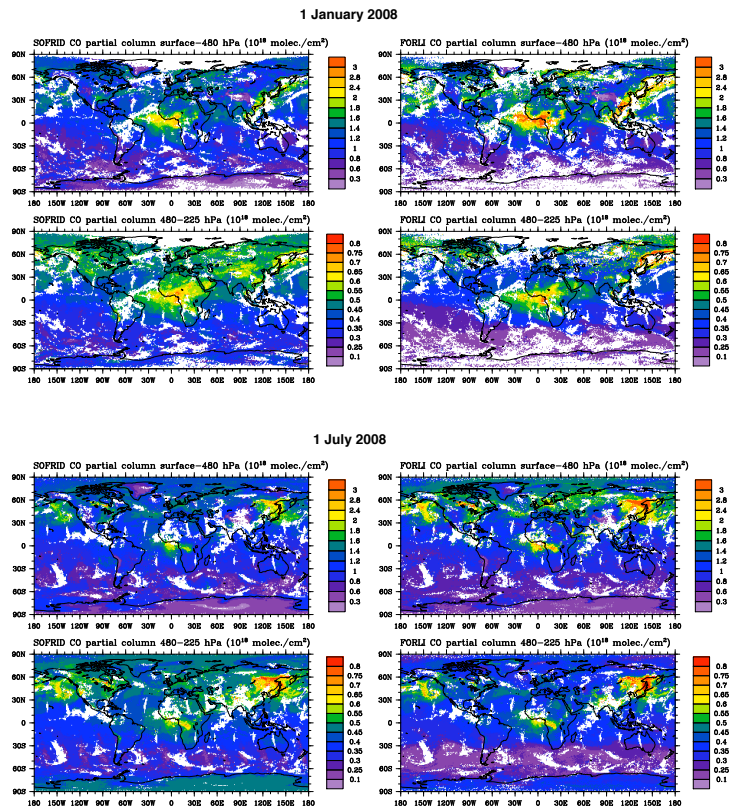
Fig. 4. Global plots of CO partial columns (surface-480 hPa and 480–225 hPa) retrieved with SOFRID (left panels) and FORLI (right panels) for 1 January 2008 (top panels) and 1 July 2008 (bottom panels), representing the global CO distribution during two composite seasons. Shown here are daily means (average of the daytime and nighttime observations). The pixels are binned on a 1° × 1° grid.

Title Page

Abstract | Introduction

Conclusions | References

Tables | Figures

◄ | ►

◄ | ►

Back | Close

Full Screen / Esc

Printer-friendly Version

Interactive Discussion
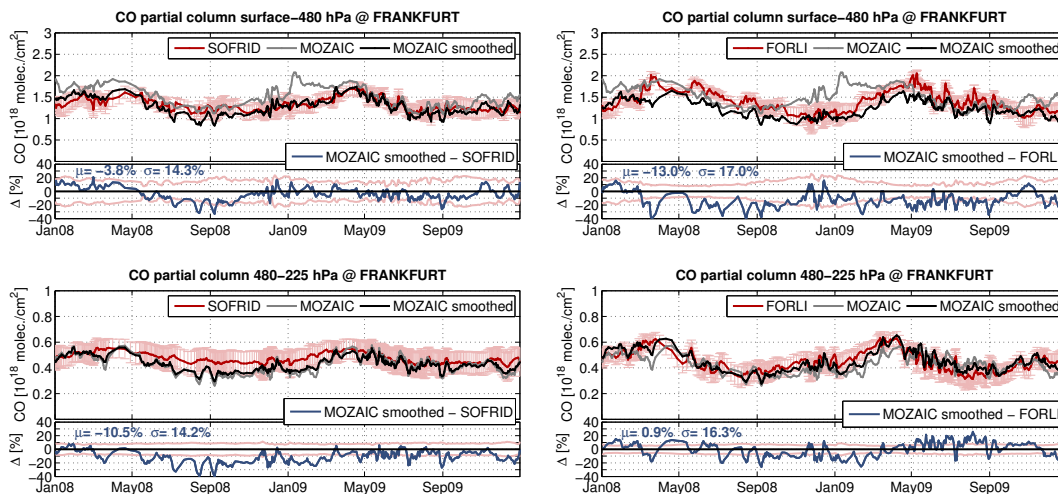
Fig. 5. Temporal variation of lower (surface-480 hPa) (top panels) and upper tropospheric (480–225 hPa) (bottom panels) partial columns at Frankfurt of MOZAIC versus SOFRID (left panels) and FORLI (right panels). IASI retrieved partial columns are given in red, MOZAIC partial columns in grey and MOZAIC data smoothed with the averaging kernels of the respective IASI algorithm (SOFRID left, FORLI right) in black. The pink vertical bars represent the IASI partial column retrieval error. The relative difference between smoothed MOZAIC and IASI (MOZAIC-IASI/((MOZAIC + IASI)/2), in percentage) is given below each figure in blue, with its mean (μ) and standard deviation (σ). The pink contours represent the IASI retrieval error. The data is smoothed by a 5-point moving average.
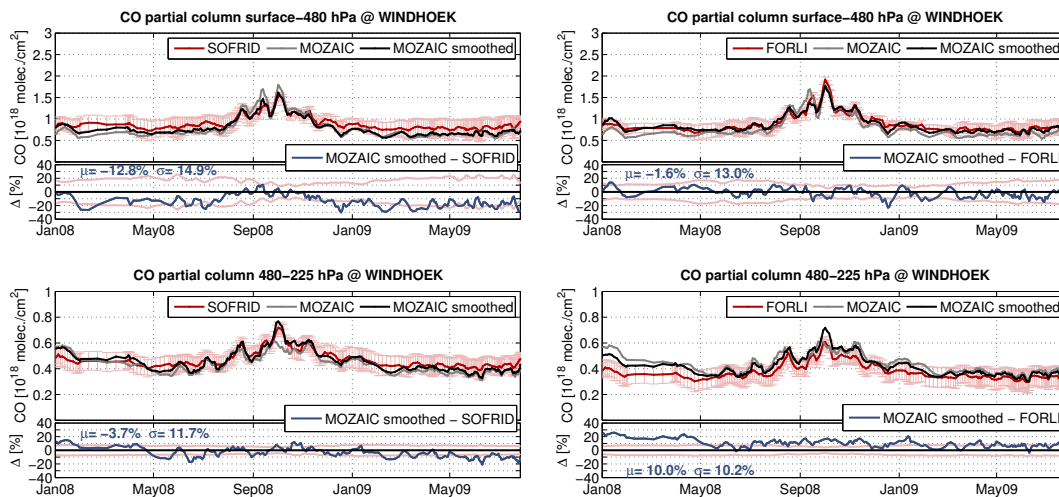
Fig. 6. As in Fig. 5 for Windhoek. Note the different timescale (MOZAIC flights to Windhoek stopped in July 2009).

Title Page

Abstract | Introduction

Conclusions | References

Tables | Figures

◄ | ►|

◄ | ►

Back | Close

Full Screen / Esc
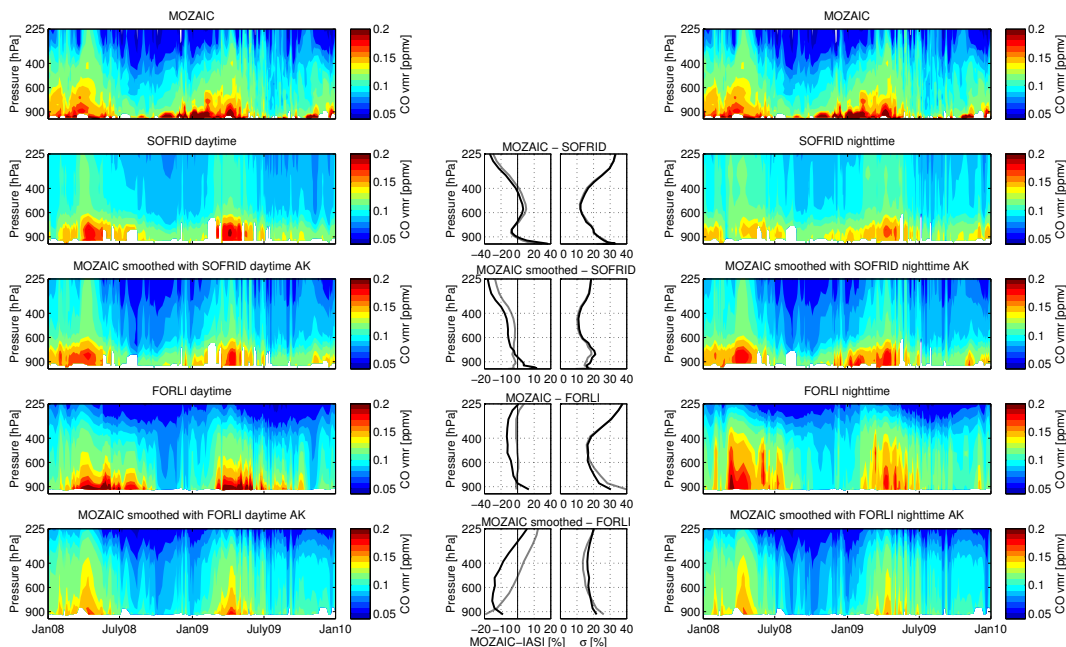
Printer-friendly Version

Interactive Discussion

Fig. 7. Left panels: temporal variation of CO profiles at Frankfurt for the years 2008–2009, as observed by (from top to bottom panels) MOZAIC, daytime SOFRID, MOZAIC convolved with SOFRID daytime averaging kernels (AK), daytime FORLI and MOZAIC convolved with FORLI daytime AK. A 5-point moving average was applied. (middle) Normalised mean differences between MOZAIC and IASI profiles (MOZAIC-IASI/((MOZAIC + IASI)/2)) and standard deviation (σ), for daytime (grey) and nighttime (black) retrievals, in percentage. Right panels: as the 5 figures on the left, but for IASI nighttime retrievals. Note, the time series of the raw MOZAIC profiles at Frankfurt is presented twice (the top left and right panels are identical).
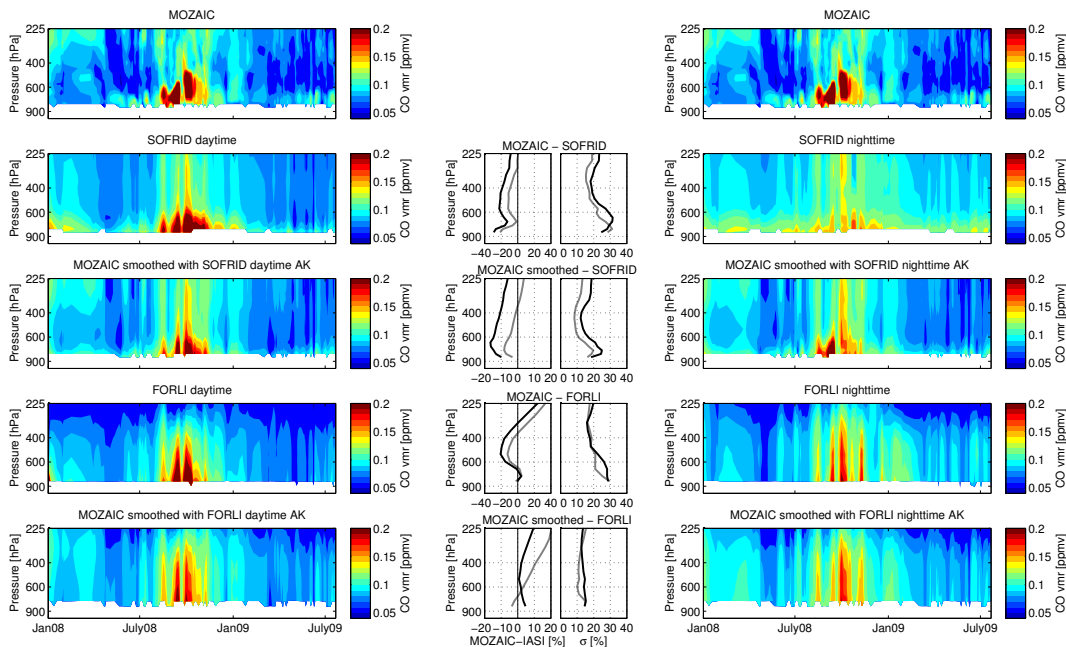
Fig. 8. As Fig. 7 for Windhoek from January 2008 to July 2009.